

RSC Advances

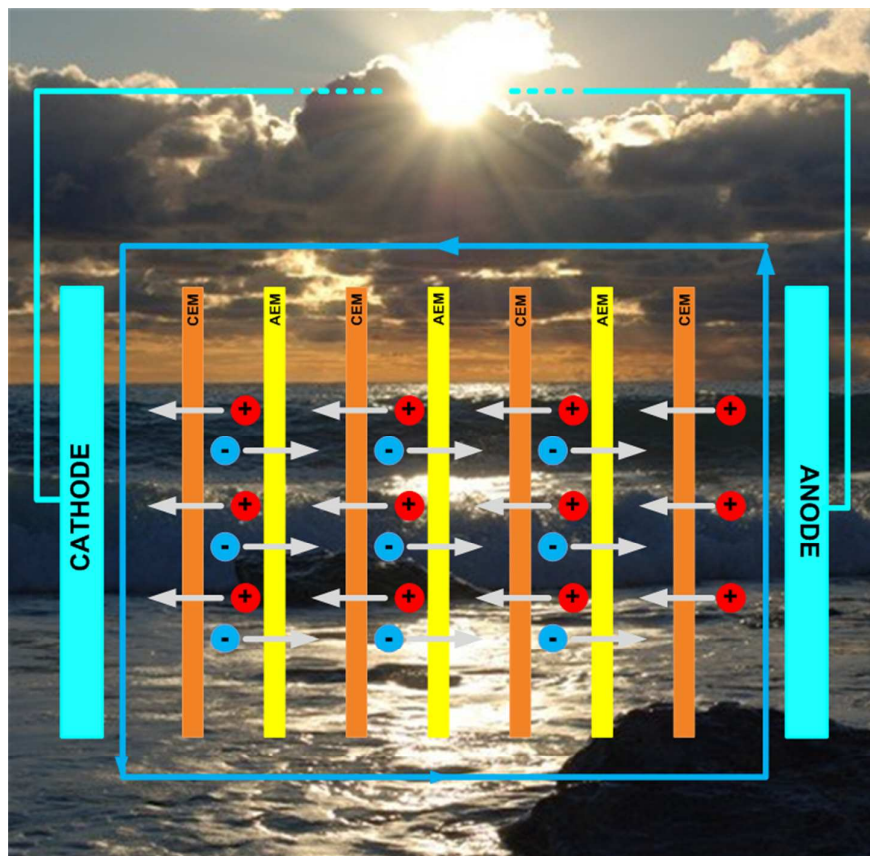


This is an *Accepted Manuscript*, which has been through the Royal Society of Chemistry peer review process and has been accepted for publication.

Accepted Manuscripts are published online shortly after acceptance, before technical editing, formatting and proof reading. Using this free service, authors can make their results available to the community, in citable form, before we publish the edited article. This *Accepted Manuscript* will be replaced by the edited, formatted and paginated article as soon as this is available.

You can find more information about *Accepted Manuscripts* in the [Information for Authors](#).

Please note that technical editing may introduce minor changes to the text and/or graphics, which may alter content. The journal's standard [Terms & Conditions](#) and the [Ethical guidelines](#) still apply. In no event shall the Royal Society of Chemistry be held responsible for any errors or omissions in this *Accepted Manuscript* or any consequences arising from the use of any information it contains.



Salinity Gradient Power-Reverse Electrodesis (SGP-RE), tested for the production of electrical energy from brackish water and solar pond brine, resulted in maximum power density of 1.13 W/m^2 cell pair, that is 63% less than the value measured using NaCl solutions with comparable salinity.

Cite this: DOI: 10.1039/c0xx00000x

www.rsc.org/advances

ARTICLE

Potential of brackish water and brine for energy generation by salinity gradient power-reverse electro dialysis (SGP-RE)

Ramato Ashu Tufa^a, Efrem Curcio^{a,b,*}, Willem van Baak^c, Joost Veerman^d, Simon Grasman^d, Enrica Fontananova^b, Gianluca Di Profio^b

Received (in XXX, XXX) Xth XXXXXXXXXX 20XX, Accepted Xth XXXXXXXXXX 20XX

DOI: 10.1039/b000000x

In the present work, a salinity gradient power-reverse electro dialysis (SGP-RE) unit was tested for the production of electrical energy by exploiting the chemical potential of real brackish water and exhaust brine from solar pond. A cross-flow SGP-RE module (REDstack B.V.), equipped with AEM-80045 and
 10 CEM-80050 membranes specifically developed by Fujifilm Manufacturing Europe B.V. within the EU-funded project REAPOWERS (“Reverse Electro dialysis Alternative Power Production”), was able to generate a maximum power density (expressed in Watts per m² Membrane Pair - MP) of 3.04 W/m²_{MP} when operated with pure NaCl aqueous solutions (0.1M in Low Concentration Compartment - LCC, 5M in High Concentration Compartment - HCC) at 20°C and recirculation rate of 20 l/h. However, a drastic
 15 reduction to 1.13 W/m² (-63%) was observed when feeding SGP-RE unit with artificial multi-ion solutions mimicking real brackish water and exhaust brine. Further experimental activity allowed at identifying Mg²⁺ ion as responsible for the significant increase in stack resistance and consequent depletion in SGP-RE performance. Therefore, specific softening treatments of the real solutions should be considered in order to maintain the process efficiency at practical level.

20

Introduction

Global demand for energy is increasing at unsustainable rate mainly due to global economic expansion, population growth and increasing living standard in emerging countries. As a result, the
 25 extensive utilization of available fossil fuels is causing a progressive depletion of these resources and an increase in global CO₂ emission. Renewable energy sources with limited thermal and environmental pollution, and absence of net emission of greenhouse gases and radioactive wastes, are attracting a growing
 30 attention. In particular, Reverse Electro dialysis (RE) is an emerging technology having the potential to generate energy from salinity power gradients (SGP). In a typical SGP-RE module, Cation Exchange Membranes (CEM) and Anion Exchange Membranes (AEM) are stacked alternately in a
 35 module; driven by a concentration gradient, the diffusive flux of ions generates an electrochemical membrane potential recorded as a voltage across electrodes¹. From a theoretical point of view, the value of the voltage from unloaded RE stack (Open Circuit Voltage - OCV) is predicted by the following equation²:

40

$$OCV = \frac{2NRT}{F} \left[\frac{\alpha_{AEM}}{z_a} \ln \left(\frac{\gamma_{a,HCC} C_{a,HCC}}{\gamma_{a,LCC} C_{a,LCC}} \right) + \frac{\alpha_{CEM}}{z_c} \ln \left(\frac{\gamma_{c,HCC} C_{c,HCC}}{\gamma_{c,LCC} C_{c,LCC}} \right) \right] \quad (1)$$

where R is the universal gas constant (8.314 J·mol⁻¹K⁻¹), N the number of membrane pairs, T the temperature (K), z the valence,
 45 α the average transport number of counter-ions, F the Faraday constant (96485 C/mol), γ the activity coefficient of the ion, and C the concentration (mol/l); subscripts a, c, HCC and LCC refer to anion, cation, High Concentration Compartment and Low Concentration Compartment, respectively.

50 Previous investigations carried out on aqueous NaCl solutions, mimicking seawater and river water salinity, reached a power density around 2 W/m² of membrane³⁻⁷ and energy efficiency around 50%⁸. Vermaas et al. (2013) showed that the theoretical obtainable Gibbs free energy of mixing seawater (30 g/l NaCl)
 55 and river water (1 g/l NaCl), both at flow rate of 1 m³/s, is 1.39 MW⁸.

Advantages from SGP-RE operations carried out at high concentration in the HCC have been clearly envisaged in the work of Post et al. (2008): if LCC and HCC are fed with 0.05M
 60 and 5 M NaCl, respectively, the theoretically available amount of energy from mixing 1m³ of diluted and 1m³ of a concentrated solution at 293 K increases to 15 MJ⁹.

At present, literature works on RE systems operated under high
 65 concentrated solutions like brine are scarce in number and, in large part, refer to pure NaCl aqueous solutions. A power density up to 0.87 W/m² (all data are referred to total membrane area, unless otherwise specified) has been reported for a RE system

operated with a standard grade electro dialysis membrane compartments filled with a coal-mine brine and fresh water¹⁰. Theoretical models predict that a power density up to 8.5 W/m² is achievable by appropriate optimization and use of specially developed AEM and CEM membranes contacted with brine and seawater solutions¹. However, the behaviour of a RE system might vary significantly when operated with real solutions. From equation (1) it is possible to roughly envisage the different levels of influence of monovalent and multivalent ions on the open circuit voltage generated by SGP-RE: assuming apparent membrane permselectivity and activity coefficients constant, the electrochemical potential generated by monovalent ions (almost all investigations in literature focus on Na⁺ and Cl⁻) is about twice as large as the one produced by divalent ions (Mg²⁺ and Ca²⁺ are among the most abundant ions in natural water) when operating at equal ion concentration ratio. Therefore, the sensitivity of SGP-RE system to real feed conditions is crucial for practical applications.

So far, literature lacks systematic and adequate information on the effect of simultaneous presence of ions other than sodium and chloride on SGP-RE performance. Vermaas et al. (2014) observed that, when using a mixture with a molar fraction of 10% MgSO₄ and 90% of NaCl in both LCC and HCC, experimentally obtained power density in steady state decreased from 29% to 50% compared to the case where the feed solutions contained only NaCl as a salt¹¹. An increase of stack resistance due to addition of Mg²⁺ ions into sodium chloride solution was also noticed by Post et al. (2009)¹². More experimental investigation is needed in order to define clearly the potentialities of SGP-RE technology and to move a decisive step towards real applications.

In the present work, with the aim to investigate realistic high-salinity conditions, where sodium, magnesium, calcium, chloride, sulfate, and bicarbonate are among the most common and abundant salt ions in natural waters, experiments have been carried out using brackish water and brine from solar ponds (Sicily, Italy) as sources for low concentration compartment (LCC) and high concentration compartment (HCC) of a SGP-RE unit, respectively. The effect of ionic composition on SGP-RE was evaluated by measurement of current, voltage and power density.

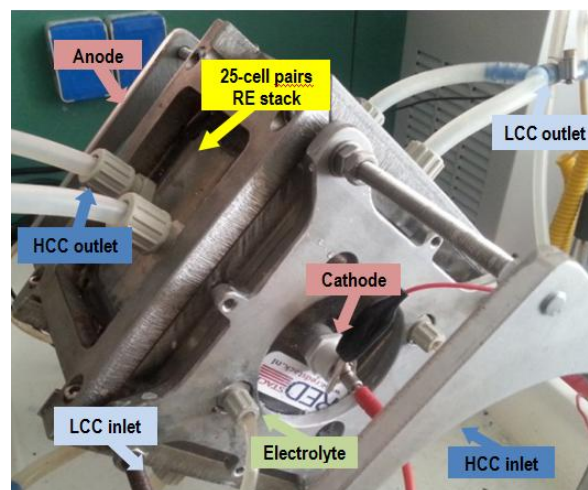
Materials and methods

Reverse electro dialysis stack

Experimental tests were carried out on a SGP-RE stack (Figure 1.a) provided by REDstack B.V (The Netherlands). The stack, operating in a cross-flow configuration, has an active membrane area of 0.01m² (10 cm x 10 cm) and 25 cell pairs. The module was equipped with 270 μm poly-ethylene gaskets and PET spacers (Deukum GMBH, Germany). Anode and cathode made of inert Ti-Ru/Ir mesh had a dimension of 10cm×10cm (MAGNETO Special Anodes B.V., The Netherlands). All experiments were carried out at 20°C.

55

a)



b)

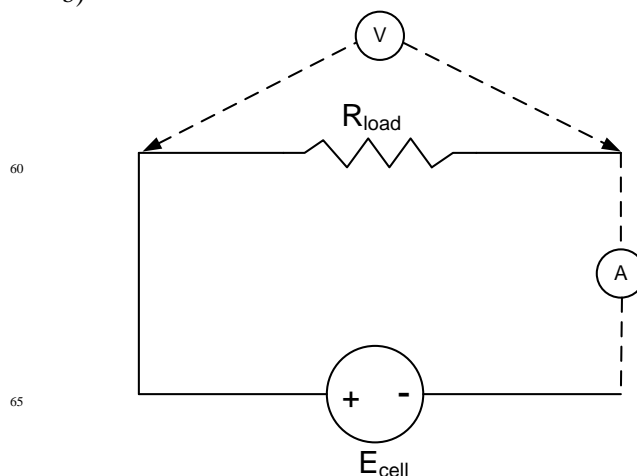


Figure 1.a The cross-flow stack used in SGP-RE experiments. Figure 1.b. Electric circuit diagram of the experimental apparatus. The ammeter (A) is connected in series and voltmeter (V) connector in parallel with the resistance box (R_{load}).

70

Membranes

Ion Exchange Membranes (IEM) used are AEM-80045 and CEM-80050 provided by Fujifilm Manufacturing Europe B.V (The Netherlands). The membranes were activated in a 0.1 M NaCl solution before use and stored with the same solution in the stack during intervals of the testing periods. Membrane characteristics are summarized in Table 1¹³.

Electrolyte and testing solutions

The electrolyte solution, recirculated throughout the electrolytic compartments at 30 l/h by Masterflex L/S digital peristaltic pumps (Cole-Palmer, US), was prepared by dissolving potassium

hexacyanoferrate (II), potassium hexacyanoferrate (III) and sodium chloride (Sigma-Aldrich S.r.l., Italy) in de-ionized water (PURELAB, Elga LabWater®, 0.055 $\mu\text{S}/\text{cm}$) up to a final concentration of 0.3M $\text{K}_4\text{Fe}(\text{CN})_6$, 0.3M $\text{K}_3\text{Fe}(\text{CN})_6$ and 2.5M NaCl.

Table 1. Relevant properties of ion exchange membranes¹³

Membrane code	Thickness (μm) †	Ion exchange capacity (mmol/g membrane)	Density of fixed charges (mol/L) †	Membrane areal resistance ($\Omega \text{ cm}^2$) ‡
Fuji-AEM-80045	129±2	1.4±0.1	3.8±0.2	1.551±0.001
Fuji-CEM-80050	114±2	1.1±0.1	2.4±0.2	2.974±0.001

† Measurement conditions: NaCl 0.5 M, 20 °C.

‡ Measurement conditions: NaCl 0.5 M, 20°C, 2.8 cm S^{-1} .

10

Testing solutions (composition in Table 2) were prepared by dissolving in de-ionized water the following salts in reagent grade: NaHCO_3 , KCl and Na_2SO_4 purchased from Sigma Aldrich S.r.l. (Italy); NaCl, $\text{CaCl}_2 \cdot 2\text{H}_2\text{O}$ and $\text{MgCl}_2 \cdot 6\text{H}_2\text{O}$ from Carlo Erba Reagenti (Italy).

15

Salt solutions were recirculated throughout the SGP-RE system at flowrate of 20 l/h by Masterflex L/S digital peristaltic pumps Mod. N. 7528-10 6-600 rpm (Cole-Palmer, US). Heated circulating baths (PolyScience, US) were used to control the temperature of recirculating streams; temperature at the six inlets of the module was monitored by Multi-channel datalogging thermometers type K 800024 with high full scale accuracy of +/- 0.5% rdg (Sper Scientific, US). Conductivity of solutions was measured by YSI (US) model 3200 Conductivity Instrument.

Table 2. Ion composition of real brackish water and brine from solar pond (20°C). Source: Ettore Infersa evaporation salt pond (Sicily, Italy).

		Na^+	K^+	Ca^{2+}	Mg^{2+}	Cl^-	HCO_3^-	SO_4^{2-}
Brackish water	Concentration (mg/l)	1520	49.7	101	323	3560	0.523	335
	Molar ratio		$[\text{Na}^+]/[\text{K}^+] = 52.1$	$[\text{Na}^+]/[\text{Ca}^{2+}] = 26.4$	$[\text{Na}^+]/[\text{Mg}^{2+}] = 4.99$		$[\text{Cl}^-]/[\text{HCO}_3^-] = 11717$	$[\text{Cl}^-]/[\text{SO}_4^{2-}] = 28.8$
Brine from Solar Pond	Concentration (mg/l)	66000	7740	242	37400	170000	50.0	64400
	Molar ratio		$[\text{Na}^+]/[\text{K}^+] = 14.5$	$[\text{Na}^+]/[\text{Ca}^{2+}] = 474$	$[\text{Na}^+]/[\text{Mg}^{2+}] = 1.86$		$[\text{Cl}^-]/[\text{HCO}_3^-] = 5841$	$[\text{Cl}^-]/[\text{SO}_4^{2-}] = 7.15$
	Theoretical voltage over membrane (mV)†	84	117	5	61	80	122	42

† calculated from eq. (1). Activity coefficients calculated by PHREEQC v. 2.18.00 software¹⁵

30 Electrochemical measurements

A high dissipation five decade resistance box in the range of 0.1-1000 Ω (CROPICO, Bracken Hill, US) was used to load the SGP-RE system. DC voltage drop across the load resistors was measured by a 3½ digital multimeter with accuracy of $\pm 0.5\%$ in

the range of range 200 mV-200 V (Valleman, DVM760), and the current flowing across the load resistors by Agilent 34422A 6½ Digit Multimeter, according to scheme provided in Figure 1.b. All measurements were carried out under continuous operation. The performance of SGP-RE unit was evaluated in terms of voltage (V), current (I) and power density (P_d). The experimental points V vs I were fit by a straight line having equation:

$$V(I) = OCV - R_{stack} \cdot I \quad (2)$$

where Open Circuit Voltage OCV is evaluated at the intersection of V(I) with the voltage axis (I=0), and R_{stack} is the stack resistance (the slope of the straight line). The intercept of V(I) with the current axis (V=0) represents the shortcut current $I_{shortcut}$. The calculated electric power density P_d (expressed in terms of W/m^2 of AEM and CEM pair) plotted as a function of the current density i shows a typical parabolic trend.

It is noteworthy to mention that power density is equal to zero when the current is equal to zero (open circuit condition) or when the voltage is equal to zero (shortcut condition).

Ion chromatography (IC) was used to evaluate the variation in composition of LCC dilute solutions after one hour of SGP-RE operation in batch mode.

Cation and anion analysis was performed by 861 Advanced Compact Ion Chromatograph (Metrohm Italiana SrL, Italy) and data processed by ICNet 2.3 software. For cation analysis, Metrosep A Supp 5 250/4.0 column and Metrosep A Supp 4/5 Guard pre-column were used with eluent solution 2mM HNO_3 /0.25 mM Oxalic Acid; for anion analysis, METROSEP C4 - 250/4.0 column and METROSEP C 4 Guard pre-columns were used, with 3.2 mM Na_2CO_3 /1 mM NaHCO_3 as eluent solution.

65

Results and discussion

70 Reference test with NaCl

SGP-RE performance was preliminarily checked by feeding

aqueous NaCl solutions (LCC: 0.1M; HCC: 5M). According to Figure 2.a, the measured OCV was 3.4 V and $I_{\text{shortcut}}=0.89$ A. The power density curve shown in Figure 2.b is fitted by equation (3) for $a=1.52 \cdot 10^{-3}$ and $b=0.136$. Under these conditions, the system was able to provide a maximum gross power density of 3.04 W/m^2 in correspondence of a current density of 44.7 A/m^2 . The maximum gross power density generated under these conditions was assumed as a reference for the system operated with multi-ion solutions.

Kim and Logan (2011) showed that an innovative microbial reverse-electrodialysis unit (5-cells stack), when operated with typical seawater (600 mM NaCl) and river water (12 mM NaCl) solutions at 0.85 mL/min, produced up to 3.6 W/m^2 (cathode surface area) and 1.2-1.3 V with acetate as a substrate; a higher flowrate (1.55 mL/min) resulted in power densities up to 4.3 W/m^2 .

In a comparative study between reverse electrodialysis and pressure retarded osmosis, both considered for applications on seawater and river water, Post et al. (2007) calculated a potential maximum power density for SGP-RE in the range of 2-4 W/m^2 . Using a 50-cells stack, a power density of 0.93 W/m^2 was obtained by Veerman and colleagues (2009) with artificial river water (1 g/l NaCl) and artificial sea water (30 g/l NaCl).

Daniilidis et al. (2014) achieved a power density of 6.7 W/m^2 of total membrane area using 0.01 M NaCl solution against 5M at 60°C; in general, the power density was found to increase monotonically for high concentrated feed solutions.

Theoretical predictions on a 12-cells stack equipped with Fujifilm ion exchange membranes and operated with 0.5M/5.4M NaCl diluate/concentrate solutions resulted in a maximum gross power density of 2.4 W/m^2 . A maximum gross power density of 2.2 W/m^2 was measured in a stack having an inter-membrane distance of 100 μm using 0.507M NaCl as artificial seawater and 0.017 M NaCl as artificial river water.

Tests on brackish water / solar pond brine

SGP-RE performance was then evaluated using artificial brackish water (fed to LCC) and exhaust brine from solar pond (fed to HCC) according to composition detailed in Table 2. Experimental data reported in Figure 2.a-b show a significant reduction of the maximum gross power density generated by the SGP-RE stack; taking as a reference the value of 3.04 W/m^2 (recorded when operating with pure NaCl solutions), it was found that $P_{d,\text{max}}$ decreased down to 1.13 W/m^2 in correspondence of a current density of 20.1 A/m^2 when operating with artificial brackish water/brine solutions. Moreover, the -63% power density reduction was accompanied by an increase of stack resistance by 76% (from 3.83 to 6.76 Ω), while OCV and shortcut current fell down to 2.77 V and 0.41 A, respectively.

Effect of other ions

In order to discriminate the effect of multiple ions on the drastic reduction of power density generated by SGP-RE unit operated with real solutions, the combined effect of each single cation

(X^{U+}) and anion (Y^{S-}) in presence of NaCl was investigated, and binary solutions were prepared according to compositions reported in Table 3. The ratios $[\text{Cl}^-]/[\text{Y}^{S-}]$ and $[\text{Na}^+]/[\text{X}^{U+}]$ within solutions fed to LCC and HCC were kept the same as in brackish water and brine, respectively. The trend of voltage, current and power density when SGP-RE was operated with multi-ion solutions is shown in Figure 3.a-b. The observed effect of HCO_3^- on SGP-RE performance was negligible due to the very low concentration of bicarbonate ion in both LCC ($8.5 \cdot 10^{-6}$ M) and HCC ($8.5 \cdot 10^{-4}$ M). As a result, the OCV remained substantially unchanged (3.39 V) as well as I_{shortcut} (0.89 A) and $P_{d,\text{max}}$ (3.03 W/m^2).

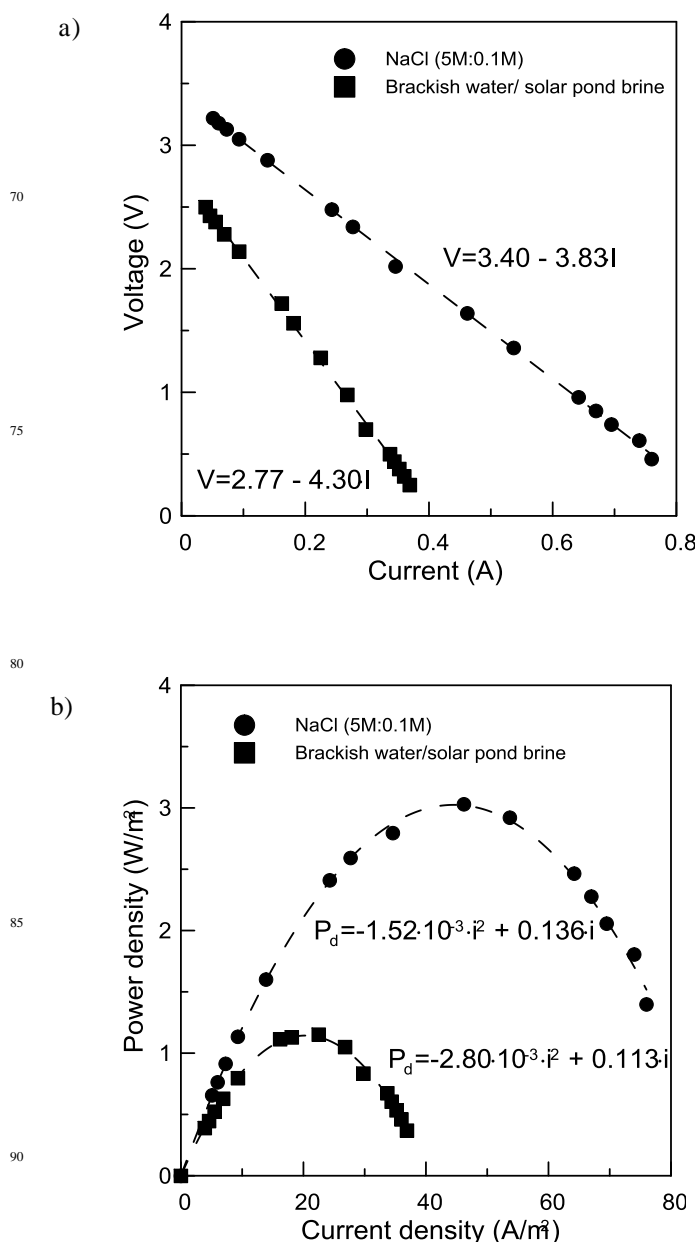


Figure 2: a) Voltage vs current; b) gross power density vs current density. Data collected under reference conditions: NaCl solution (0.1M/0.5M). Temperature: 20°C. Margin of error within 10%.

Despite its significant concentration in the brine (0.32 M), the impact of K^+ on the power density was quite limited due to the similar electrochemical properties between Na^+ and K^+ ions: ionic radii of unhydrated Na^+ and K^+ are 1.17 Å and 1.64 Å, respectively; ionic radii of hydrated Na^+ and K^+ are 3.58 Å and 3.32 Å, respectively¹⁸; ion diffusion coefficients in water for Na^+ and K^+ are $1.334 \cdot 10^{-9} \text{ m}^2/\text{s}$ and $1.957 \cdot 10^{-9} \text{ m}^2/\text{s}$, respectively¹⁹. While no appreciable difference in OCV was observed, I_{shortcut} moderately decreased to 0.83 A (-6.7%) and R_{stack} increased to 4.08 Ω (+6.5%). The maximum power density (2.84 W/m²) was reached for a current density of 41.8 A/m².

Table 3. Molar composition of binary LCC/HCC solutions used to investigate the effect of individual ions in presence of NaCl.

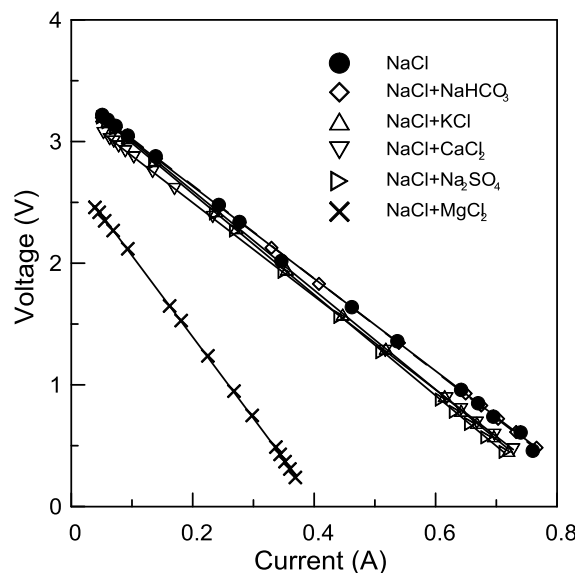
LCC solution composition	HCC solution composition	Parameters in equation (2)	
		OCV (V)	R_{stack} (Ω)
0.1 M NaCl	5 M NaCl	3.40	3.83
0.0999975 M NaCl + $8.5 \cdot 10^{-6}$ M NaHCO ₃ $[Cl^-]/[HCO_3^-] = 11717$	4.99915 M NaCl + $8.5 \cdot 10^{-4}$ M NaHCO ₃ $[Cl^-]/[HCO_3^-] = 5841$	3.39	3.79
0.098 M NaCl + 0.002 M KCl $[Na^+]/[K^+] = 52.1$	4.68 M NaCl + 0.32 M KCl $[Na^+]/[K^+] = 14.5$	3.40	4.08
0.096 M NaCl + 0.004 M CaCl ₂ $[Na^+]/[Ca^{2+}] = 26.4$	4.99 M NaCl + 0.01 M CaCl ₂ $[Na^+]/[Ca^{2+}] = 474$	3.27	3.84
0.0966 M NaCl + 0.0034 M Na ₂ SO ₄ $[Cl^-]/[SO_4^{2-}] = 28.8$	4.39 M NaCl + 0.61 M Na ₂ SO ₄ $[Cl^-]/[SO_4^{2-}] = 7.15$	3.40	4.15
NaCl 0.083 M + MgCl ₂ 0.017 M $[Na^+]/[Mg^{2+}] = 4.99$	NaCl 3.25 M + MgCl ₂ 1.75 M $[Na^+]/[Mg^{2+}] = 1.86$	2.73	6.69

Due to its propensity to form sparingly soluble CaSO₄ and to precipitate from solution, Ca²⁺ is generally present in natural waters only at relatively low concentration. As a consequence, for the investigated LCC/HCC composition of 0.004M /0.096M CaCl₂, both OCV and power density were affected in a limited extent (-4% and -6.6 % with respect to pure NaCl, respectively). Sulphate and magnesium ions typically have the highest concentration after Na⁺ and Cl⁻ in brine, seawater and brackish water. However, the presence of SO₄²⁻ did not change significantly OCV and resulted in a moderate decrease of I_{shortcut} (0.82 A) and $P_{d,\text{max}}$ (2.79 W/m², - 8.2% with respect to pure NaCl).

On the other hand, the presence of magnesium decreased

drastically both OCV (2.73 V, -20% with respect to pure NaCl) and power density (1.11 W/m², -64 % with respect to pure NaCl). The value of $i_{P_{d,\text{max}}} = 20.2 \text{ A/m}^2$ was the lowest measured. The effect of magnesium valence on the reduced electrical potential difference has been already anticipated when introducing the equation (1).

a)



b)

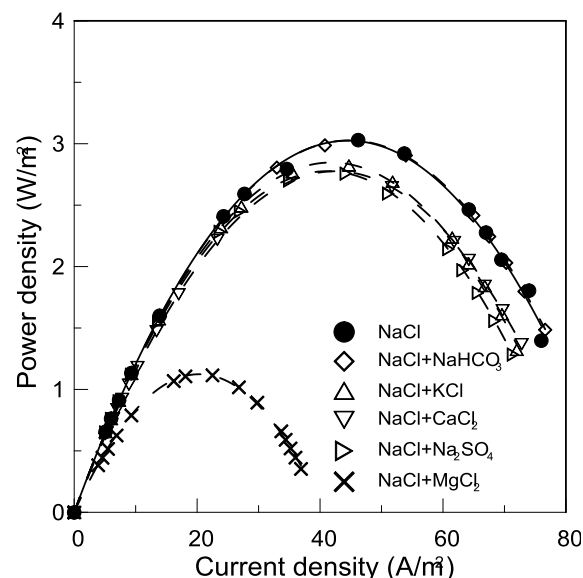


Figure 3. a) Voltage vs current; b) gross power density vs current density for multi-ion solutions. Compositions are detailed in Table 3. Temperature: 20°C. Margin of error within 10% (average of 3 tests).

Moreover, the significant enhancement of cell resistance might be ascribed to an increase of membrane resistance in presence of Mg²⁺. Sata (2004) reported a two to three-fold increase in electrical resistance for different commercial cation exchange membranes (NEOSEPTA CL-25T, AMFion C-310, Ionac MC-

3470) when using MgCl_2 instead of NaCl . An enhancement of the electrical resistance of membranes with the concentration of the electrolyte solution was also due to the increase in Donnan adsorbed salts and shrinking of the membranes.²⁰

A systematic investigation of this aspect, based on Electrochemical Impedance Spectroscopy¹³⁻¹⁴, will be object of future communications.

Stack resistance

A significant advantage gained when operating SGP-RE at high salt concentration is the reduction of the electrical resistance compared to the extensively studied case of low salt concentration (i.e. combination river water/seawater). The extent of the Internal Area Resistance (IAR) per cell for the different tested solutions is presented in Figure 4.

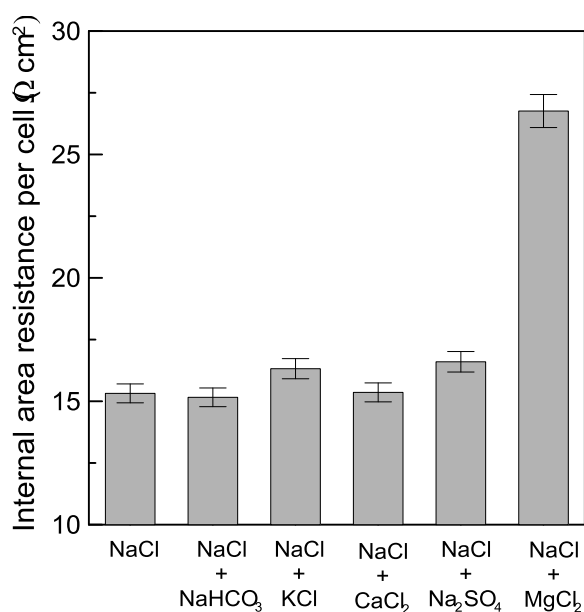


Figure 4. Internal area resistance per cell for the binary solutions investigated (single membrane area: 100 cm^2 ; number of cell pairs: 25).

These results show a lower IAR per cell of SGP-RE stack (below $26.8 \text{ } \Omega\text{cm}^2$) compared to previous investigations on RE operated with river water/seawater solutions pair which was above $50 \text{ } \Omega\text{cm}^2$ in most cases^{3-4, 18}. With respect to reference NaCl solutions ($R_{\text{stack}}=3.83 \text{ } \Omega$, $\text{IAR}= 15.32 \text{ } \Omega\text{cm}^2$), significant variations in electrical resistance were observed only for $\text{NaCl} + \text{MgCl}_2$ solutions. In this case, the presence of magnesium increased by 75% the resistance of the stack ($6.69 \text{ } \Omega$) and IAR ($26.8 \text{ } \Omega\text{cm}^2$), resulting in a drastic decrease of power density by 64 %.

Transport of ions

Ion chromatography was used to check the variation of ion composition in feed solutions as a result of the migration of ions through IEM driven by an electrochemical potential. Experimental tests were carried out in batch mode by recycling both artificial brackish water and artificial brine over the stack under open-

circuit conditions (absence of net flux of electrical charges) and collecting samples after 1 hour.

Only solution flowing in the low concentration compartment was analyzed, due to the large measurement errors related to the small variations in the highly concentrated brine.

Table 4. Ion composition (from Ion Chromatography analysis) of the low-concentration stream in SGP-RE batch operation (LCC: artificial brackish water; HCC: artificial brine).

Ion	HCC		LCC	
	Initial concentration (mg/l)	Initial concentration (mg/l)	Concentration after 1 hour (mg/l)	Concentration increase (mmol/l)
Na^+	66000	1520	3870	102
K^+	7740	49.7	478	11
Mg^{2+}	37400	323	1740	58
Ca^{2+}	242	101	115	0.35
Cl^-	170000	3560	8960	152
SO_4^{2-}	64400	335	3380	32

Volume of low conc. compartment: 5 L; volume of high conc. compartment: 5 L. Solutions recirculated at 20 l/h. Temperature: 20°C .

Data averaged on 3 measurements.

Results reported in Table 4 show an increase in the overall concentration of LCC in the investigated interval of time, and the total mass of dissolved ions increases by 164% from 6970 to 18400 mg/l. Within a narrow margin of measurement error (2%), the charge balance after migration of ions is satisfied (total positive charge = 329 meq/l; total negative charge = 323 meq/l). Figure 5 illustrates the transport rate of each ion as a function of its concentration in HCC compartment.

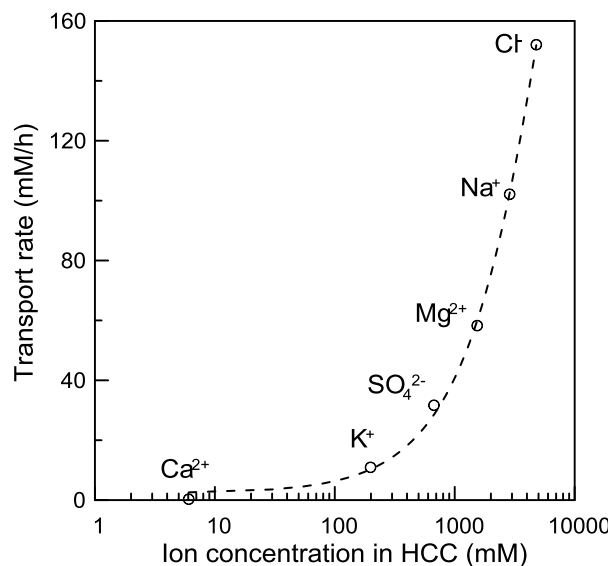


Figure 5. Transport rate of single ions versus their concentration in brine compartment.

Due to the non-ideal behavior of membranes, having selectivity lower than 100%, a combined transport of both

cations and anions can occur. It is interesting to compare transport rate and theoretical voltage over membrane for each ion reported in Table 2. The measured OCV for the SGP-RE stack operated with brackish water/solar pond brine was 2.77V (Figure 2.a), thus implying a membrane voltage of 55 mV. Most of the voltages reported in Table 2 are higher than 55 mV, indicating a forward transport. Exceptions are for divalent ions Ca^{2+} and SO_4^{2-} , where expected back-transport is not observed due to the effect of multiple co-ion transport. When considering all ions, the overall electrochemical balance is satisfied within an acceptable confidence interval (7%).

Diffusion of Na^+ resulted in a concentration increase of 155% for an initial HCC/LCC Na^+ concentration ratio of 34; a similar concentration increase (+152%) was found for chlorine with an initial HCC/LCC Cl^- concentration ratio of 47.8. These data seem to confirm that ion migration through ion exchange membranes is substantially driven by a concentration gradient. In highlighting experiments on ion transport carried out by Post et al. (2009), where the LCC solution consisted of 3 mM NaCl + 2 mM MgSO_4 and the HCC of 0.45 M NaCl+0.05 M MgSO_4 , a almost twofold increase of sodium and chloride content in the LCC was observed after one hour when operating with standard-grade ion-exchange membranes¹².

Moreover, our measurements indicate that sodium and magnesium are transported across CEM with a flux of 2.84 and 3.24 meq/m²s, respectively, while chlorine and sulfate diffuse across AEM with rate 4.23 and 1.76 meq/m²s, respectively.

Conclusions

A cross-flow SGP-RE stack equipped with AEM-80045 and CEM-80050 membranes, when operated with 0.1 M/5M NaCl solutions, reached a maximum gross power density of 3.04 W/m² at 20°C and recirculation rate of 20 l/h. However, a remarkable increase of stack resistance (+75%) and a significant loss of maximum power density (-64%) were observed when the SGP-RE was operated with feed solutions containing Mg^{2+} ions (HCC: NaCl 3.25 M + MgCl_2 1.75 M; $[\text{Na}^+]/[\text{Mg}^{2+}] = 1.86$; LCC: NaCl 0.083 M + MgCl_2 0.017 M; $[\text{Na}^+]/[\text{Mg}^{2+}] = 4.99$). The comparable decrease in power density observed for artificial multi-ion solutions mimicking brackish water and exhaust brine from solar pond (Ettore Inferna site, Sicily), depicts the necessity for specific softening strategies for a better performance of SGP-RE under real conditions. In this respect, the integration of SGP-RE within pre-treatment schemes of typical SWRO desalination plants might represent a feasible and economically viable option for recovering the electrochemical energy intrinsically present into discharged brines.

Moreover, an urgent need for developing specific ion exchange membranes not suffering from magnesium effects is envisaged.

Acknowledgement

The financial support of European Union within the project REAPower – “Reverse Electrodialysis Alternative Power Production” under the EU-FP7 programme (Project No. 256736, www.reapower.eu), and the financial support of The Education,

Audiovisual and Culture Executive Agency (EACEA) under the Program “Erasmus Mundus Doctorate in Membrane Engineering” - EUDIME (FPA 2011-0014, http://eudime.unical.it), are kindly acknowledged.

Notes and references

^aDepartment of Environmental and Chemical Engineering, University of Calabria (DIATIC-UNICAL) via P. Bucci CUBO 45A, 87036 Rende (CS) Italy

^bInstitute on Membrane Technology of the National Research Council (ITM-CNR), c/o University of Calabria Via P. Bucci, cubo 17/C, 87036 Rende (CS), Italy

^cFujifilm Manufacturing Europe B.V., Oudenstaart 1, 5047 TK Tilburg, The Netherlands

^dREDstack B.V., Pieter Zeemanstraat 6, 8606 JR Sneek, The Netherlands

*Corresponding author: e.curcio@unical.it; tel: +39 0984 494013; fax: +39 0984 496655

1. M. Tedesco, A. Cipollina, A. Tamburini, W. van Baak and G. Micale, *Desalination and Water Treatment*, 2012, **49**, 404-424.
2. L. F. Weinstein JN, *Science*, 1976, **191**, 557-559.
3. P. Dlugolecki, A. Gambier, K. Nijmeijer and M. Wessling, *Environmental Science and Technology*, 2009, **43**, 6888-6894.
4. J. Veerman, M. Saakes, S. J. Metz and G. J. Harmsen, *Journal of Membrane Science*, 2009, **327**, 136-144.
5. J. W. Post, C. H. Goeting, J. Valk, S. Goinga, J. Veerman, H. V. M. Hamelers and P. J. F. M. Hack, *Desalination and Water Treatment*, 2010, **16**, 182-193.
6. J. Veerman, M. Saakes, S. J. Metz and G. J. Harmsen, *Environmental Science and Technology*, 2010, **44**, 9207-9212.
7. D. A. Vermaas, M. Saakes and K. Nijmeijer, *Environmental Science & Technology*, 2011, **45**, 7089-7095.
8. D. A. Vermaas, J. Veerman, N. Y. Yip, M. Elimelech, M. Saakes and K. Nijmeijer, *ACS Sustainable Chemistry & Engineering*, 2013, **1**, 1295-1302.
9. J. W. Post, J. Veerman, H. V. M. Hamelers, G. J. W. Euverink, S. J. Metz, K. Nijmeijer and C. J. N. Buisman, *Journal of Membrane Science*, 2007, **288**, 218-230.
10. M. Turek, B. Bandura and P. Dydó, *Desalination*, 2008, **221**, 462-466.
11. D. A. Vermaas, J. Veerman, M. Saakes and K. Nijmeijer, *Energy & Environmental Science*, 2014.
12. J. W. Post, H. V. M. Hamelers and C. J. N. Buisman, *Journal of Membrane Science*, 2009, **330**, 65-72.
13. E. Fontananova, W. Zhang, I. Nicotera, C. Simari, W. van Baak, G. Di Profio, E. Curcio and E. Drioli, *Journal of Membrane Science*, 2014, **459**, 177-189.
14. P. Dlugolecki, P. Ogonowski, S. J. Metz, M. Saakes, K. Nijmeijer, and M. Wessling, *J. Membrane Sci.*, 2010, **349**, 369-379
15. D. L. Parkhurst and C. A. L. Appelo, *US Geol.Surv. Water Res. Invest. Rep.*, 1999, **99-4259**, 1-312.
16. Y. Kim and B. E. Logan, *Environ. Sci. Technol.*, 2011, **45**, 5834-5839.

-
17. A. Daniilidis, D.A. Vermaas, R. Herber and K. Nijmeijer, *Renewable Energy*, 2014, **64**, 123-131.
 18. A. G. Volkov, S. Paula and D. W. Deamer, *Bioelectrochemistry and Bioenergetics*, 1997, **42**, 153-160.
 - 5 19. E. Samson, J. Marchand and K. A. Snyder, *Mat. Struct.*, 2003, **36**, 156-165.
 20. T. Sata, *Ion Exchange Membrane*. Royal Society of Chemistry, Cambridge (UK) 2004
 - 10 21. J. W. Post, H. V. M. Hamelers and C. J. N. Buisman, *Environmental Science and Technology*, 2008, **42**, 5785-5790.